Simultaneous Active-Passive Beamformer Design in IRS-Enabled Multi-Carrier DFRC System

Tong Wei, Linlong Wu, Kumar Vijay Mishra, Bhavani Shankar M. R.
Interdisciplinary Centre for Security, Reliability and Trust (SnT), University of Luxembourg
email: {tong.wei@, linlong.wu@, kumar.mishra@ext., bhavani.shankar@}uni.lu

***Abstract*—Intelligent reflecting surfaces (IRS) are increasingly considered as an enabling technology for non-line-of-sight (NLoS) communications and remote sensing. We consider an IRS-aided dual-function radar-communications (DFRC) system for multi-carrier waveforms in a combined light-of-sight and NLoS scenario. In this wideband system, we jointly design the radar receive filter, frequency-dependent beamforming, and IRS phases to maximize the average radar signal-to-interference-plus-noise ratio (SINR) and the minimal communications SINR among all users. The problem has a maximin objective function with constant modulus and power constraints and is, therefore, highly non-convex. We solve this optimization using the alternating maximization framework, which iterates amongst the alternating direction method of multipliers, Riemannian steepest descent, and Dinkelbach's algorithms. Numerical experiments demonstrate that the proposed method for IRS-aided DFRC achieves better performance for both sensing and communications than the system without IRS.**

***Index Terms*—Alternating maximization, dual-function radar-communications, intelligent reflecting surfaces.**

I. Introduction

Recently, intelligent reflecting surfaces (IRS) have attracted considerable research interest in the communications and sensing communities [1, 2]. IRS comprises many low-cost reconfigurable elements that control the phase of the impinging signal [3]. The near passive behavior and low cost of IRS compared to conventional relays have the potential for massive deployment to improve the wireless propagation without additional energy consumption [4, 5]. This has led to a surge in research on applications that may benefit from IRS, including wireless communications [6, 7] and remote sensing [8, 9].

Initial investigations of IRS were limited to wireless communications [10–14]. These studies used IRS to compensate for the end-to-end path loss, i.e., transmitter-IRS and IRS-receiver channels. The transmit power from the base station was minimized while guaranteeing a minimum signal-to-interference-plus-noise ratio (SINR) for each user. Some recent works have explored IRS to enhance the detection and estimation performance of radar systems [8, 9, 15–17]. The IRS-aided radar system has been shown to exploit additional echoes from a target to improve the probability of detection [8]. To improve the intensity of the return signal, IRS may be closely deployed to the receive antennas of MIMO radar [15]. Meanwhile, the signal-to-noise ratio (SNR) could be maximized through carefully designing phases of reflecting elements [16]. Novel radar surveillance models with the assistance of a single IRS has been proposed for non-line-of-sight (NLoS) sensing scenario [17]. Here, to further expand the coverage region, IRS is deployed at suitable positions to build the extra line-of-sight (LoS) path between transmitter and receiver.

Recently, spectral crowding has led to the development of dual-function radar-communications (DFRC) systems that share both hardware and spectral resources [18, 19]. The flexibility of multi-beam control has driven the utilization of IRS in such DFRC systems to enhance sensing and/or communications functionalities [20–22]. Both passive and active beamforming could be jointly devised for the IRS-aided DFRC to enhance the radar detection performance while ensuring the single-user SNR [22]. Further, the multiple transmit beams of the dual-function base station (DFBS) may be aligned to the target directions [21]. Meanwhile, with the assistance of the IRS, multi-user interference (MUI) is eliminated to guarantee the quality of service. However, in this scheme, IRS is used only to improve communications performance. Note that the aforementioned IRS-assisted DFRC systems emit narrowband signals with the limited achievable rates.

Contrary to previous work [22], we focus on integrating IRS into wideband multi-carrier DFRC system. Meanwhile, our previous work [23] introduced wideband IRS-assisted DFRC, which was limited in the NLoS scenario. In this paper, both the LoS and NLoS paths are considered to further enhance the performance of sensing and communications. In particular, we consider orthogonal frequency division multiplexing (OFDM) signaling for the DFRC and jointly optimize the performance of both radar and communications. By simultaneously designing the radar receive filter, active (i.e., transmit precoding matrix) and passive (i.e., IRS phase-shift matrix) beamformers, we aim to maximize the radar SINR and the minimum communications SINR simultaneously. The resulting non-convex optimization problem is solved through the alternating maximization (AM) framework. Numerical results illustrate the effectiveness and superiority of the proposed design approach.

The rest of the paper is organized as follows. In the next section, we introduce the system model for wideband IRS-aided DFRC system and formulate the problem. We describe our optimization procedure in Section III and validate it through numerical experiments in Section IV. We conclude in Section V. Throughout this paper, we denote the vectors and matrices by boldface lowercase and uppercase letters, respectively. Then, $(\cdot)^T$, $(\cdot)^*$ and $(\cdot)^H$ denote transpose, conjugate, and Hermitian transpose, respectively; $\mathbf{I}_L$ denotes the $L \times L$ identity matrix; $\|\cdot\|_2$ and $\|\cdot\|_F$ are the ℓ_2 and Frobenius norms, respectively.

II. Signal Model

Consider an IRS-assisted wideband OFDM-DFRC system (Fig. 1) that consists of an N_t-antenna dual-function transmitter, an N_r-antenna radar receiver and a single IRS comprising N_m reflecting elements. Herein, the transmitter and receiver antennas are uniform linear arrays (ULAs) and closely deployed with the DFBS. The transmit signal is composed of OFDM symbols, with the symbol duration $\triangle t$, modulated to spread over K subcarriers. Denote the normalized transmit data symbol at the k-th subcarrier as $\mathbf{s}_k = [s_{k,1}, \cdots, s_{k,U}]^T \in \mathbb{C}^{U\times 1}$, where $k = 1, \cdots, K$ and $\mathbb{E}\{\mathbf{s}_k\mathbf{s}_k^H\} = \mathbf{I}_U$. To overcome spatial wideband effect known as beam squint [24], we utilize the frequency-dependent digital beamforming $\mathbf{F}_k \in \mathbb{C}^{N_t\times U}$ to precode the data symbol such that the signal $\mathbf{F}_k\mathbf{s}_k \in \mathbb{C}^{N_t\times 1}$ is transmitted on the k-th subcarrier. Utilizing the N_t K-point inverse fast Fourier transform (IFFT), the transmit baseband signal is

$$\mathbf{x}(t) = \sum_{k=1}^{K} \mathbf{F}_k\mathbf{s}_k e^{\jmath 2\pi f_k t}, \tag{1}$$

where t denotes the time instant, $f_k = (k-1)\triangle f$ denotes the baseband frequency at the k-th subcarrier with $\triangle f$ being the frequency step of OFDM signaling. To guarantee the orthogonality of each subcarrier, the frequency step-size is set as $\triangle f = 1/\triangle t$.

On the other hand, for wideband DFRC, the transmit power should meet the system requirement, i.e.,

$$\|\mathbf{F}_k\|_F^2 \le P_k, \tag{2}$$

where P_k denotes the maximum power assigned to the k-th subcarrier. The radar system aims to detect a target in the presence of Q clutter scatterers while simultaneously serving U single-antenna downlink users. We consider both the direct (i.e., LoS) and indirect (i.e., NLoS) paths for radar and communications in this system.

A. Radar model

Denote the frequency-dependent steering vectors of dual-function transmitter, radar receiver, and IRS, respectively, as

$$\begin{aligned}
\mathbf{a}_t(\theta, f_k) &= [1, e^{-jv(\theta,f_k)}, \cdots, e^{-j(N_t-1)v(\theta,f_k)}]^T,\\
\mathbf{a}_r(\theta, f_k) &= [1, e^{-jv(\theta,f_k)}, \cdots, e^{-j(N_r-1)v(\theta,f_k)}]^T,\\
\mathbf{b}(\theta, f_k) &= [1, e^{-jv(\theta,f_k)}, \cdots, e^{-j(N_m-1)v(\theta,f_k)}]^T,
\end{aligned}$$

where $v(\theta, f_k) = 2\pi(f_k + f_c)(\frac{d\sin(\theta)}{c})$. After sampling the signal and applying N_r K-point fast Fourier transform (FFT), the radar receive signal at the k-th subcarrier is

$$\begin{aligned}
\mathbf{Y}(f_k) =& \mathbf{A}_k\mathbf{F}_k\mathbf{s}_k + \boldsymbol{E}_k(\boldsymbol{\Phi})\mathbf{F}_k\mathbf{s}_k\\
&+ \widetilde{\mathbf{A}}_k\mathbf{F}_k\mathbf{s}_k + \widetilde{\boldsymbol{E}}_k(\boldsymbol{\Phi})\mathbf{F}_k\mathbf{s}_k + \mathbf{n}_r(f_k),
\end{aligned} \tag{3}$$

where $\mathbf{A}_k = \alpha_1\mathbf{a}_r^H(\theta_{d,t}, f_k)\mathbf{a}_t^H(\theta_{d,t}, f_k)$ denotes the target response matrix for direct path (i.e., Tx- target-Rx); $\boldsymbol{E}_k(\boldsymbol{\Phi}) = \mathbf{E}_k\boldsymbol{\Phi}\mathbf{G}_k + \mathbf{D}_k\boldsymbol{\Phi}\mathbf{B}_k + \mathbf{D}_k\boldsymbol{\Phi}\mathbf{W}_k\boldsymbol{\Phi}\mathbf{G}_k$ denotes the indirect path (i.e., Tx-IRS-target-Rx, Tx-target-IRS-Rx and Tx-target-IRS-target-Rx), respectively; α_1 is the corresponding direct path gain; $\mathbf{G}_k$, $\mathbf{W}_k$, $\mathbf{D}_k$, $\mathbf{B}_k$ and $\mathbf{E}_k$ are the channel matrices between Tx-IRS, IRS-IRS, IRS-Rx, Tx-target-IRS, IRS-target-Rx, respectively; and $\boldsymbol{\Phi}$ is the phase shift matrix of IRS. Similarly, $\widetilde{\mathbf{A}}_k$ and $\widetilde{\boldsymbol{E}}_k$ denote the clutter response matrix for direct path and indirect path, respectively, wherein we omit the steering vectors and angles, because of paucity of space. Hereafter, all angles of arrival/departure are measured with respect to (w.r.t.) the array broadside direction and are positive when moving clockwise.

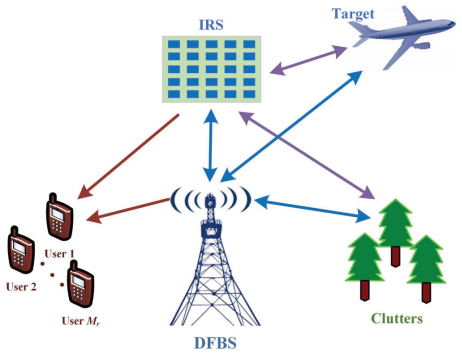

Figure 1. Illustration of an IRS-aided DFRC. The DFBS has both LoS and NLoS paths to the radar target and communications users.

Define the average SINR of radar over all subcarriers as

$$\mathrm{SINR}_r = \frac{\sum_{k=1}^{K}|\mathbf{w}^H(\mathbf{A}_k + \boldsymbol{E}_k(\boldsymbol{\Phi}))\mathbf{F}_k\mathbf{s}_k|^2}{\sum_{k=1}^{K}|\mathbf{w}^H(\widetilde{\mathbf{A}}_k + \widetilde{\boldsymbol{E}}_k(\boldsymbol{\Phi}))\mathbf{F}_k\mathbf{s}_k|^2 + K\sigma_r^2\mathbf{w}^H\mathbf{w}}, \tag{4}$$

where $\mathbf{w}$ is the receive filter bank and σ_r^2 denotes the noise power of radar at each subcarrier.

B. Communications model

Denote the channel state information (CSI) matrix from transmitter to all users at the k-th subcarrier as $\mathbf{H}_k \in \mathbb{C}^{U\times N_t}$. Note that the CSI could be estimated and hence, we assume it is known in advance. The received baseband signal of all the user is

$$\mathbf{Y}_k(t) = \mathbf{H}_k\mathbf{F}_k\mathbf{s}_k e^{\jmath 2\pi f_k t} + \widetilde{\mathbf{H}}_k\boldsymbol{\Phi}\mathbf{G}_k\mathbf{F}_k\mathbf{s}_k e^{\jmath 2\pi f_k t} + \mathbf{n}_{c,k}(t), \tag{5}$$

where $\widetilde{\mathbf{H}}_k$ denotes the CSI from IRS to the user. We transfer the received signal to frequency domain using U K-point FFT. Then, the received signal of the u-th user at the k-th subcarrier is

$$\begin{aligned}
\mathbf{Y}_u(f_k) =& \mathbf{h}_{u,k}^T\mathbf{f}_{k,u}s_{k,u} + [\tilde{\mathbf{h}}_{u,k}^T\boldsymbol{\Phi}\mathbf{G}_k\mathbf{f}_{k,u}s_{k,u}\\
&+ \sum_{i\neq u}\mathbf{h}_{u,k}^T\mathbf{f}_{k,i}s_{k,i} + \sum_{i\neq u}\tilde{\mathbf{h}}_{u,k}^T\boldsymbol{\Phi}\mathbf{G}_k\mathbf{f}_{k,i}s_{k,i}] + \mathbf{n}_k(u),
\end{aligned} \tag{6}$$

where $\tilde{\mathbf{h}}_{u,k} \in \mathbb{C}^{N_m\times 1}$ is the channel between the u-th user and IRS, $\mathbf{f}_{k,u}$ is the u-th column of $\mathbf{F}_k$, and $\mathbf{n}_k(u)$ is the noise of u-th user. According to (6), the average signal power of the u-th user over all K subcarriers is

$$P_u = \sum_{k=1}^{K}\| \underbrace{(\mathbf{h}_{u,k}^T + \tilde{\mathbf{h}}_{u,k}^T\boldsymbol{\Phi}\mathbf{G}_k)}_{\mathbf{z}_{k,u}(\boldsymbol{\Phi})}\mathbf{F}_k\boldsymbol{\Lambda}_u\|_2^2, \tag{7}$$

where $\mathbf{\Lambda}_u$ is the diagonal selection matrix with only the u-th element being one and the rest being zero. Meanwhile, the average power of MUI at the u-th user is

$$P_{MUI} = \sum_{k=1}^{K} \|\mathbf{z}_{k,u}(\mathbf{\Phi})\mathbf{F}_k\bar{\mathbf{\Lambda}}_u\|_2^2, \tag{8}$$

where $\bar{\mathbf{\Lambda}}_u$ is the diagonal matrix with only the u-th diagonal element being zero and the rest being one. Then, it follows that the SINR at the u-th users is

$$\mathrm{SINR_u} = \frac{\sum_{k=1}^{K} \|\mathbf{z}_{k,u}(\mathbf{\Phi})\mathbf{F}_k\mathbf{\Lambda}_u\|_2^2}{\sum_{k=1}^{K} \|\mathbf{z}_{k,u}(\mathbf{\Phi})\mathbf{F}_k\bar{\mathbf{\Lambda}}_u\|_2^2 + K\sigma_c^2}, \tag{9}$$

where σ_c^2 denotes the noise power of communications user which is constant over all subcarriers.

C. Problem formulation

To improve both sensing and communications performances, the radar SINR and the minimal communications SINR among all users should be maximized simultaneously. The resulting optimization problem is

$$\begin{aligned} \underset{\mathbf{w},\mathbf{\Phi},\mathbf{F}_k}{\text{maximize}} \quad & \mathrm{SINR}_r + \min_u\{\mathrm{SINR}_u\} \\ \text{subject to} \quad & \|\mathbf{F}_k\|_F^2 \le P_k, \forall k, \\ & |\mathbf{\Phi}(i,i)| = 1, \forall i, \end{aligned} \tag{10}$$

where P_k denotes the maximal transmit power at the k-th subcarrier. Then, the problem in (10) is equivalently reformulated as

$$\begin{aligned} \underset{\eta,\mathbf{w},\mathbf{\Phi},\mathbf{F}_k}{\text{maximize}} \quad & \mathrm{SINR}_r + \eta \\ \text{subject to} \quad & \mathrm{SINR}_u \ge \eta, \forall u \\ & \|\mathbf{F}_k\|_F^2 \le P_k, \forall k \\ & |\mathbf{\Phi}(i,i)| = 1, \forall i, \end{aligned} \tag{11}$$

where η denotes the auxiliary variable of the threshold of communications SINR. The problem in (11) has a fractional quartic objective function with constant modulus and difference of convex (DC) constraints and is, therefore, highly non-convex. To tackle (11), we devise an alternating maximization (AM) based approach in the sequel.

III. Optimization Method

Within the AM framework, at each iteration, we solve the following four subproblems related to (11).

A. Update of receive filter $\mathbf{w}$

For a given transmit beamforming $\mathbf{F}_k$ and phase-shift $\mathbf{\Phi}$, the subproblem w.r.t. receive filter bank $\mathbf{w}$ is

$$\underset{\mathbf{w}}{\text{maximize}} \ \frac{\mathbf{w}^H\mathbf{\Upsilon}_t\mathbf{w}}{\mathbf{w}^H\mathbf{\Upsilon}_c\mathbf{w} + K\sigma_r^2\mathbf{w}^H\mathbf{w}}, \tag{12}$$

where

$$\mathbf{\Upsilon}_t = \sum_{k=1}^{K}(\mathbf{A}_k + \boldsymbol{E}_k(\mathbf{\Phi}))\mathbf{F}_k\mathbf{F}_k^H(\mathbf{A}_k + \boldsymbol{E}_k(\mathbf{\Phi}))^H, \tag{13}$$

and

$$\mathbf{\Upsilon}_c = \sum_{k=1}^{K}(\widetilde{\mathbf{A}}_k + \widetilde{\boldsymbol{E}}_k(\mathbf{\Phi}))\mathbf{F}_k\mathbf{F}_k^H(\widetilde{\mathbf{A}}_k + \widetilde{\boldsymbol{E}}_k(\mathbf{\Phi}))^H. \tag{14}$$

Note that the problem in (12) is different from the conventional the minimum variance distortionless response (MVDR) because of the summation matrix $\mathbf{\Upsilon}_t$. Hence, it does not directly yield a closed-form solution. Using Charnes-Cooper transformation [25], problem (12) becomes

$$\underset{\mathbf{w}}{\text{minimize}} \ \mathbf{w}^H\widetilde{\mathbf{\Upsilon}}_c\mathbf{w} \quad \text{subject to } \mathbf{w}^H\mathbf{\Upsilon}_t\mathbf{w} = 1, \tag{15}$$

where $\widetilde{\mathbf{\Upsilon}}_c = \mathbf{\Upsilon}_c + K\sigma_r^2\mathbf{I}$. The problem in (15) consists of a complex-valued homogeneous QCQP, which is non-convex because of the quadratic equality constraint. Semidefinite relation (SDR) yields

$$\begin{aligned} \underset{\mathbf{W}}{\text{minimize}} \quad & \mathrm{Tr}(\widetilde{\mathbf{\Upsilon}}_c\mathbf{W}) \\ \text{subject to} \quad & \mathbf{W} \succeq \mathbf{0}, \mathrm{Tr}(\mathbf{\Upsilon}_t\mathbf{W}) = 1. \end{aligned} \tag{16}$$

It follows from [26] that the optimal solution $\mathbf{W}^\star$ for the problem in (16) is rank-1 and hence, the SDR is tight. Therefore, the solution of problem (15) is $\mathbf{W}^\star = \mathbf{w}^\star\mathbf{w}^{\star H}$.

B. Update of precoding matrices $\mathbf{F}_k$

With the fixed t, $\mathbf{w}$, and $\mathbf{\Phi}$, the corresponding optimization problem is

$$\begin{aligned} \underset{\boldsymbol{f}\in\mathbb{C}^{KN_tU\times 1}}{\text{maximize}} \quad & \frac{\boldsymbol{f}^H\mathbf{\Xi}_t\boldsymbol{f}}{\boldsymbol{f}^H\mathbf{\Xi}_c\boldsymbol{f} + K\sigma_r^2\mathbf{w}^H\mathbf{w}} \\ \text{subject to} \quad & \|\mathbf{V}_k\boldsymbol{f}\|_2^2 \le P_k, \forall k, \\ & \frac{\boldsymbol{f}^H\mathbf{R}_u\boldsymbol{f}}{\boldsymbol{f}^H\bar{\mathbf{R}}_u\boldsymbol{f} + K\sigma_c^2} \ge \eta, \forall u, \end{aligned} \tag{17}$$

where $\boldsymbol{f} = [\mathrm{vec}(\mathbf{F}_1)^T, \cdots, \mathrm{vec}(\mathbf{F}_K)^T]^T$ and $\mathbf{V}_k$ denotes the selection matrix to extract k-th interval of $\boldsymbol{f}$. Owing to the paucity of space, we omit the detailed expression of semidefinite matrices $\mathbf{\Xi}_t$, $\mathbf{\Xi}_c$, $\mathbf{R}_u$ and $\bar{\mathbf{R}}_u$, which can be directly derived from (4) and (9). Note that, for the function $f(\mathbf{x}) = \mathbf{x}^H\mathbf{H}\mathbf{x}$, the following inequality is always satisfied

$$f(\mathbf{x}) \ge 2\Re(\mathbf{x}_n^H\mathbf{H}\mathbf{x}) - f(\mathbf{x}_n), \tag{18}$$

where $\mathbf{H}$ is positive semidefinite Hermitian matrix, $\mathbf{x}_n$ denotes the current point, and the equality holds if and only if $\mathbf{x} = \mathbf{x}_n$.

Using the inequality in (18), we linearize and reformulate the objective function and constraint of (17) as

$$\begin{aligned} \underset{\boldsymbol{f}}{\text{maximize}} \quad & \frac{2\Re(\boldsymbol{f}_n^H\mathbf{\Xi}_t\boldsymbol{f}) - \boldsymbol{f}_n^H\mathbf{\Xi}_t\boldsymbol{f}_n}{\boldsymbol{f}^H\mathbf{\Xi}_c\boldsymbol{f} + K\sigma_r^2\mathbf{w}^H\mathbf{w}} \\ \text{subject to} \quad & \|\mathbf{V}_k\boldsymbol{f}\|_2^2 \le P_k, \forall k, \\ & \eta\boldsymbol{f}^H\bar{\mathbf{R}}_u\boldsymbol{f} - 2\Re(\boldsymbol{f}_n^H\mathbf{R}_u\boldsymbol{f}) \le \text{const.}, \forall u, \end{aligned} \tag{19}$$

where const. $= -\eta K\sigma_c^2 - \boldsymbol{f}_n^H\mathbf{R}_u\boldsymbol{f}_n$, and $\boldsymbol{f}_n$ denotes the value in last iteration. This problem is tackled by Dinkelbach's algorithm [27] as the following lemma.

Lemma 2: Given $f(\mathbf{x})$ and $g(\mathbf{x})$ as a non-negative concave and a convex function, respectively, over a convex set $\mathcal{X}$. Then, the fractional programming problem

$$\underset{\mathbf{x}}{\text{maximize}} \ \frac{f(\mathbf{x})}{g(\mathbf{x})} \quad \text{subject to } \mathbf{x} \in \mathcal{X}, \tag{20}$$

is solved via Dinkelbach's algorithm [28].

C. Update of phase shift matrix $\mathbf{\Phi}$

With fixed t, $\mathbf{w}$ and $\mathbf{F}_k$, the corresponding optimization problem is

$$\begin{aligned} &\underset{\boldsymbol{\phi}}{\text{maximize}} \ \frac{\bar{f}(\boldsymbol{\phi})}{\bar{g}(\boldsymbol{\phi})} \\ &\text{subject to } |\boldsymbol{\phi}(i)| = 1, \forall i \\ &\qquad \frac{q_u + 2\Re\{\boldsymbol{\phi}^H \mathbf{q}_u\} + \boldsymbol{\phi}^H \mathbf{Q}_u \boldsymbol{\phi}}{\bar{q}_u + 2\Re\{\boldsymbol{\phi}^H \bar{\mathbf{q}}_u\} + \boldsymbol{\phi}^H \bar{\mathbf{Q}}_u \boldsymbol{\phi} + K\sigma_c^2} \geq \eta, \forall u, \end{aligned} \tag{21}$$

where $\boldsymbol{\phi} = \text{diag}(\mathbf{\Phi})$, $\bar{f}(\boldsymbol{\phi})$ and $\bar{g}(\boldsymbol{\phi})$ are quartic over the variable $\boldsymbol{\phi}$. Hence, the auxiliary variable $\boldsymbol{\psi}$ is introduced to reformulate problem (20) as

$$\begin{aligned} &\underset{\boldsymbol{\phi},\boldsymbol{\psi}}{\text{maximize}} \ \bar{f}(\boldsymbol{\phi},\boldsymbol{\psi}) - \bar{\lambda}\bar{g}(\boldsymbol{\phi},\boldsymbol{\psi}) \\ &\text{subject to } \boldsymbol{\phi} = \boldsymbol{\psi} \\ &\qquad |\boldsymbol{\phi}(i)| = 1, |\boldsymbol{\psi}(i)| = 1, \forall i \\ &\qquad 2\Re(\mathbf{r}_u^H \boldsymbol{\phi}) \leq d_u, \forall u, \end{aligned} \tag{22}$$

where $\mathbf{r}_u = (\eta \boldsymbol{\phi}_t^H (\bar{\mathbf{Q}}_u - \xi_u \mathbf{I}) + \eta \bar{\mathbf{q}}_u^H - \mathbf{q}_u^H - \boldsymbol{\phi}_t^H \mathbf{Q}_u)^H$, ξ_u is the largest eigenvalue of $\bar{\mathbf{Q}}_u$, $d_u = \eta(\bar{q}_u + K\sigma_c^2 - 2\xi_u M N_m + \boldsymbol{\phi}_t^H \bar{\mathbf{Q}}_u \boldsymbol{\phi}_t) + \boldsymbol{\phi}_t^H \mathbf{Q}_u \boldsymbol{\phi}_t - q_u$, $\boldsymbol{\phi}_t$ denotes the current point of $\boldsymbol{\phi}$, $\bar{f}(\boldsymbol{\phi},\boldsymbol{\psi})$ and $\bar{g}(\boldsymbol{\phi},\boldsymbol{\psi})$ are quadratic over $\boldsymbol{\phi}$ and $\boldsymbol{\psi}$, respectively. Then, the augmented Lagrangian function of (22) is

$$\begin{aligned} \mathcal{L}(\boldsymbol{\phi},\boldsymbol{\psi},\mathbf{u},\mathbf{w},\rho) &= f(\boldsymbol{\phi},\boldsymbol{\psi},\bar{\lambda}) - \mathbf{u}^H(\boldsymbol{\phi} - \boldsymbol{\psi}) \\ &\quad - \frac{\rho}{2}\|\boldsymbol{\phi} - \boldsymbol{\psi}\|_2^2 - \sum_{u=1}^{U} w_u (2\Re(\mathbf{r}_u^H \boldsymbol{\phi}) - d_u), \end{aligned} \tag{23}$$

where $f(\boldsymbol{\phi},\boldsymbol{\psi},\bar{\lambda}) = \bar{f}(\boldsymbol{\phi},\boldsymbol{\psi}) - \bar{\lambda}\bar{g}(\boldsymbol{\phi},\boldsymbol{\psi})$, ρ is the penalty parameter, $\mathbf{u}$ and $\mathbf{w} \succeq \mathbf{0}$ denote the auxiliary variables. The alternating direction of multipliers (ADMM) updates are

$$\lambda^{(t+1)} = \frac{\bar{f}(\boldsymbol{\phi})}{\bar{g}(\boldsymbol{\phi})}, \tag{24a}$$

$$\boldsymbol{\phi}^{(t+1)} = \max_{|\boldsymbol{\phi}|=1} \mathcal{L}(\lambda^{(t+1)}, \boldsymbol{\phi}, \boldsymbol{\psi}^{(t)}, \mathbf{u}^{(t)}, \mathbf{v}^{(t)}), \tag{24b}$$

$$\boldsymbol{\psi}^{(t+1)} = \max_{|\boldsymbol{\psi}|=1} \mathcal{L}(\lambda^{(t+1)}, \boldsymbol{\phi}^{(t+1)}, \boldsymbol{\psi}, \mathbf{u}^{(t)}, \mathbf{v}^{(t)}), \tag{24c}$$

$$\mathbf{u}^{(t+1)} = \mathbf{u}^{(t)} + \rho_1(\boldsymbol{\phi}^{(t+1)} - \boldsymbol{\psi}^{(t+1)}), \tag{24d}$$

$$w_u^{(t+1)} = \text{Proj}_+(w_u^{(t)} - (2\Re(\mathbf{r}_u^H \boldsymbol{\phi}) - d_u)), \forall u. \tag{24e}$$

At each ADMM iteration, the subproblems w.r.t phase-shift $\boldsymbol{\phi}$ and $\boldsymbol{\psi}$ are solved by Riemannian steepest decent (RSD) algorithm [14].

D. Update of auxiliary variable η

For a given $\mathbf{w}$, $\mathbf{F}_k$ and $\mathbf{\Phi}$, the problem w.r.t. η is

$$\underset{\eta}{\text{maximize}} \ \eta \quad \text{subject to } \text{SINR}_u \geq \eta, \forall u. \tag{25}$$

We update $\eta = \max\{\eta_t, \arg\min_u \ \text{SINR}_u\}$, where η_t denotes the value of η at the last iteration.

IV. Numerical Experiments

Throughout all experiments, we assume both DFBS and radar receiver are equipped with a ULA with $N_t = 10$ and $N_r = 8$ elements, respectively, and located at $[0\text{m}, 0\text{m}]$ in a Cartesian coordinate system. A single target is located at $[0\text{m}, 5000\text{m}]$. The clutter scatterers are at 15° and -25°. The IRS consists of $N_m = 30$ reflecting elements deployed at $[2500\text{m}, 2500\text{m}]$. The central frequency of the wideband DFRC is 10 GHz and the subcarrier step-size is 20 MHz. We set $K = 32$ and $U = 2$. The relative element spacing for DFBS, radar receive array, and IRS are set according to the highest frequency, i.e., $d = c/2f_{max}$. The transmit power constraints at all subcarriers are identical, i.e., $P_1 = \cdots, = P_K = 10$. The beamforming matrices $\mathbf{F}_k$ and phase-shift matrices $\mathbf{\Phi}$ are initialized with the diagonal entries generated from a zero-mean Gaussian distribution. The maximum iterations for both inner and outer loops of the algorithm are set to 50.

Fig. 1(a) shows the achievable radar SINR versus the number of iterations. The proposed algorithm converges within 10 iterations. The IRS-aided radar-only system achieves the best performance because the signals from both transmitter and IRS are aligned to the target direction. When compared to non-IRS DFRC, the proposed IRS-aided DFRC yields more than 10 dB gain in radar SINR. Fig. 1(b) demonstrates the achieved minimal communications SINR against the number of iterations. Again, the proposed algorithm is convergent around 10 iterations w.r.t. minimal communications SINR. Similarly, compared with non-IRS case, the IRS-aided DFRC yield about 2.5 dB enhancement in the minimal communications SINR. Fig.1(c) shows the wideband transmit beampattern of the dual-function transmitter. The transmit energy is nearly focused toward the direction of IRS because we aim to achieve higher gain for the indirect link (i.e., IRS-aided channel). It follows that the proposed method automatically aligns the transmit beam to the direction of target or IRS.

V. Summary

In this paper, we utilize a single IRS to assist the multi-carrier DFRC system. Specifically, we aim to design both the active and passive beamforming to improve the radar SINR and the minimal communications SINR among all users, simultaneously. We develop an alternating maximization (AM) based algorithm to tackle the resulting problem. Simulation results shows that the proposed method can achieve satisfactory performance both in radar and communication.

Acknowledgment

This work was supported by the Luxembourg National Research Fund (FNR) through the SPRINGER C18/IS/12734677.

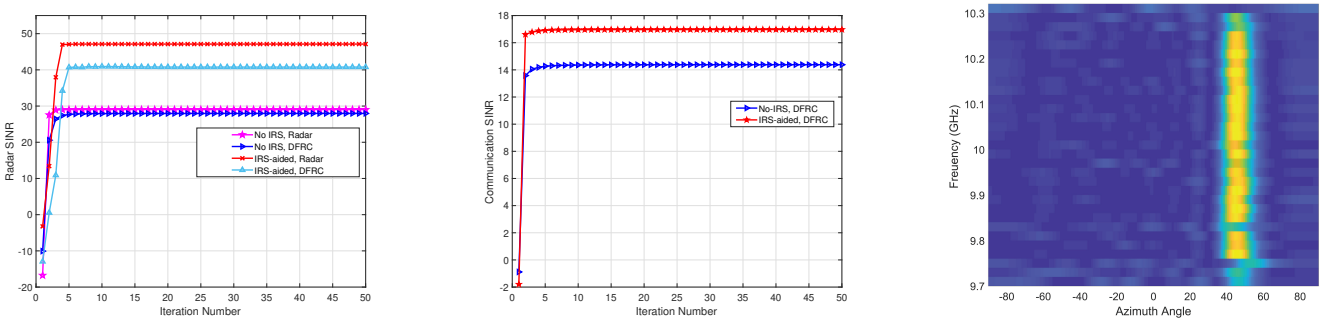

(a) (b) (c)

Figure 2. (a) Radar SINR versus number of iterations, (b) Communicationa SINR versus number of iterations, (c) Wideband transmit beampattern.

REFERENCES

[1] M. Di Renzo, A. Zappone, M. Debbah, M.-S. Alouini, C. Yuen, J. de Rosny, and S. Tretyakov, "Smart radio environments empowered by reconfigurable intelligent surfaces: How it works, state of research, and the road ahead," *IEEE Journal on Selected Areas in Communications*, vol. 38, no. 11, pp. 2450–2525, 2020.

[2] Q. Wu and R. Zhang, "Towards smart and reconfigurable environment: Intelligent reflecting surface aided wireless network," *IEEE Communications Magazine*, vol. 58, no. 1, pp. 106–112, 2020.

[3] J. A. Hodge, K. V. Mishra, and A. I. Zaghloul, "Intelligent time-varying metasurface transceiver for index modulation in 6G wireless networks," *IEEE Antennas and Wireless Propagation Letters*, vol. 19, no. 11, pp. 1891–1895, 2020.

[4] Q. Wu and R. Zhang, "Intelligent reflecting surface enhanced wireless network via joint active and passive beamforming," *IEEE Transactions on Wireless Communications*, vol. 18, no. 11, pp. 5394–5409, 2019.

[5] C. Huang, A. Zappone, G. C. Alexandropoulos, M. Debbah, and C. Yuen, "Reconfigurable intelligent surfaces for energy efficiency in wireless communication," *IEEE Transactions on Wireless Communications*, vol. 18, no. 8, pp. 4157–4170, 2019.

[6] C. Pan, H. Ren, K. Wang, W. Xu, M. Elkashlan, A. Nallanathan, and L. Hanzo, "Multicell MIMO communications relying on intelligent reflecting surfaces," *IEEE Transactions on Wireless Communications*, vol. 19, no. 8, pp. 5218–5233, 2020.

[7] M. F. Ahmed, K. P. Rajput, N. Venkategowda, K. V. Mishra, and A. K. Jagannatham, "Joint transmit and reflective beamformer design for secure estimation in IRS-aided WSNs," *IEEE Signal Processing Letters*, vol. 29, pp. 692–696, 2022.

[8] Z. Esmaeilbeig, K. V. Mishra, and M. Soltanalian, "IRS-aided radar: Enhanced target parameter estimation via intelligent reflecting surfaces," in *IEEE Sensor Array and Multichannel Signal Processing Workshop*, 2021, pp. 1–5.

[9] S. Buzzi, E. Grossi, M. Lops, and L. Venturino, "Radar target detection aided by reconfigurable intelligent surfaces," *IEEE Signal Processing Letters*, vol. 28, pp. 1315–1319, 2021.

[10] J. Liu, X. Qian, and M. Di Renzo, "Interference analysis in reconfigurable intelligent surface-assisted multiple-input multiple-output systems," in *IEEE International Conference on Acoustics, Speech and Signal Processing*, 2021, pp. 8067–8071.

[11] M. Najafi, V. Jamali, R. Schober, and H. V. Poor, "Physics-based modeling and scalable optimization of large intelligent reflecting surfaces," *IEEE Transactions on Communications*, vol. 69, no. 4, pp. 2673–2691, 2021.

[12] Z. Zhou, N. Ge, Z. Wang, and L. Hanzo, "Joint transmit precoding and reconfigurable intelligent surface phase adjustment: A decomposition-aided channel estimation approach," *IEEE Transactions on Communications*, vol. 69, no. 2, pp. 1228–1243, 2021.

[13] A. Elzanaty, A. Guerra, F. Guidi, and M.-S. Alouini, "Reconfigurable intelligent surfaces for localization: Position and orientation error bounds," *IEEE Transactions on Signal Processing*, vol. 69, pp. 5386–5402, 2021.

[14] Z. Li, M. Hua, Q. Wang, and Q. Song, "Weighted sum-rate maximization for multi-IRS aided cooperative transmission," *IEEE Wireless Communications Letters*, vol. 9, no. 10, pp. 1620–1624, 2020.

[15] W. Lu, B. Deng, Q. Fang, X. Wen, and S. Peng, "Intelligent reflecting surface-enhanced target detection in MIMO radar," *IEEE Sensors Letters*, vol. 5, no. 2, pp. 1–4, 2021.

[16] W. Lu, Q. Lin, N. Song, Q. Fang, X. Hua, and B. Deng, "Target detection in intelligent reflecting surface aided distributed MIMO radar systems," *IEEE Sensors Letters*, vol. 5, no. 3, pp. 1–4, 2021.

[17] A. Aubry, A. De Maio, and M. Rosamilia, "Reconfigurable intelligent surfaces for N-LOS radar surveillance," *IEEE Transactions on Vehicular Technology*, vol. 70, no. 10, pp. 10 735–10 749, 2021.

[18] K. V. Mishra, M. R. B. Shankar, V. Koivunen, B. Ottersten, and S. A. Vorobyov, "Toward millimeter-wave joint radar communications: A signal processing perspective," *IEEE Signal Processing Magazine*, vol. 36, no. 5, pp. 100–114, 2019.

[19] T. Wei, L. Wu, and M. R. B. Shankar, "Joint waveform and precoding design for coexistence of MIMO radar and MU-MISO communication," *IET Signal Processing*, 2022, in press.

[20] K. V. Mishra, A. Chattopadhyay, S. S. Acharjee, and A. P. Petropulu, "OptM3Sec: Optimizing multicast IRS-aided multiantenna DFRC secrecy channel with multiple eavesdroppers," in *IEEE International Conference on Acoustics, Speech and Signal Processing*, 2022, pp. 9037–9041.

[21] X. Wang, Z. Fei, Z. Zheng, and J. Guo, "Joint waveform design and passive beamforming for RIS-assisted dual-functional radar-communication system," *IEEE Transactions on Vehicular Technology*, vol. 70, no. 5, pp. 5131–5136, 2021.

[22] Z.-M. Jiang, M. Rihan, P. Zhang, L. Huang, Q. Deng, J. Zhang, and E. M. Mohamed, "Intelligent reflecting surface aided dual-function radar and communication system," *IEEE Systems Journal*, pp. 1–12, 2021.

[23] T. Wei, L. Wu, K. V. Mishra, and M. R. B. Shankar, "Multiple IRS-assisted wideband dual-function radar-communication," in *IEEE International Symposium on Joint Communications & Sensing*, 2022, pp. 1–5.

[24] M. Wang, F. Gao, S. Jin, and H. Lin, "An overview of enhanced massive mimo with array signal processing techniques," *IEEE Journal of Selected Topics in Signal Processing*, vol. 13, no. 5, pp. 886–901, 2019.

[25] A. Charnes and W. W. Cooper, "Programming with linear fractional functionals," *Naval Research Logistics Quarterly*, vol. 9, no. 3-4, pp. 181–186, 1962.

[26] Z.-Q. Luo, W.-K. Ma, A. M.-C. So, Y. Ye, and S. Zhang, "Semidefinite relaxation of quadratic optimization problems," *IEEE Signal Processing Magazine*, vol. 27, no. 3, pp. 20–34, 2010.

[27] T. Matsui, Y. Saruwatari, and M. Shigeno, "An analysis of Dinkelbach's algorithm for 0-1 fractional programming problems," Department of Mathematical Engineering and Information Physics, University of Tokyo, Japan, Tech. Rep. METR92-14, 1992.

[28] A. Aubry, A. De Maio, and M. M. Naghsh, "Optimizing radar waveform and doppler filter bank via generalized fractional programming," *IEEE Journal of Selected Topics in Signal Processing*, vol. 9, no. 8, pp. 1387–1399, 2015.